ELSEVIER

Journal of Alloys and Compounds 311 (2000) 53–56

Journal of ALLOYS AND COMPOUNDS

www.elsevier.com/locate/jallcom

XPS and voltammetric studies on $La_{1-x}Sr_xCoO_{3-\delta}$ perovskite oxide electrodes

P. Wang*, L. Yao, M. Wang, W. Wu

State Key Laboratory for Corrosion and Protection, Institute of Corrosion and Protection of Metals, The Chinese Academy of Sciences, Shenyang 110015, PR China

---

Abstract

Nonstoichiometry behavior of $La_{1-x}Sr_xCoO_{3-\delta}$ series perovskite oxides was studied by XPS and cyclic voltammetry. The results indicate that the chemical states of La and Sr in the oxides are barely influenced by their relative content. Substitution of Sr for La results in the valence state change of some cobalt ions from Co^{3+} to Co^{4+} and the increase of the lattice oxygen vacancies.

Keywords: Perovskite; Oxide electrode; XPS; Cyclic voltammetry

---

1. Introduction

Perovskite-type oxides $La_{1-x}Sr_xCoO_{3-\delta}$ are mixed electronic and ionic conductors [1]. To date, these oxides receive much attention due to their potential applications as oxidation catalysts [2], electrode materials for solid oxide fuel cells [3], gas separation membranes [4], sensor materials [5] and high-temperature superconductors [6].

The properties of the $La_{1-x}Sr_xCoO_{3-\delta}$ series perovskite oxides are associated with their high oxygen ionic diffusivity, high oxygen nonstoichiometry and high electrical conductivity. The chemical diffusion and oxygen nonstoichiometry in $La_{0.8}Sr_{0.2}CoO_{3-\delta}$ have been measured as a function of oxygen partial pressure and temperature by Lankhorst et al. [7,8] with high-temperature coulometric titration. The results show that oxygen diffusion coefficient is almost independent of oxygen partial pressure, which suggests that all oxygen vacancies contribute to oxygen ion transport in $La_{0.8}Sr_{0.2}CoO_{3-\delta}$, and oxygen nonstoichiometry is nearly independent of temperature. These results can be interpreted in terms of the itinerant electron model. For $La_{1-x}Sr_xCoO_{3-\delta}$ ($x>0.2$) [9], the itinerant electron model is valid only at low vacancy concentration, but no longer holds at high vacancy concentrations and additional ionic contribution needs to be considered.

The conduction mechanism of $La_{1-x}Sr_xCoO_{3-\delta}$ changes from semiconductor-like conduction to metal-like conduction with the increase of strontium content. The conductivity tends to decrease with x [1]. The electronic conduction of $La_{1-x}Sr_xCoO_{3-\delta}$ has generally been considered to take place by the Co 3d electrons through the chain of Co–O–Co bonds [10]. The formation of oxygen vacancy would distort the Co-6 O octahedron, weaken the crystal field around the Co ion and especially destroy the Co–O–Co electron transfer net which results in decrease of conductivity. In this work, we studied the electronic structure of $La_{1-x}Sr_xCoO_{3-\delta}$ perovskite oxides by XPS and cyclic voltammetry techniques in order to confirm this point of view.

2. Experimental

2.1. Preparation of the oxide electrodes

La–Sr–Co series perovskites were prepared by the tartaric acid-aided method. The required amounts of metal nitrates in stoichiometric ratio were dissolved in water to which tartaric acid was added. The molar ratio of acid to total metal ions was set at 2. Nickel plates (10×10×1 mm) were selected as conductive supports. Before painting, these plates were treated with oxidic acid (HCl: $H_2O_2=10:1$) for 20 min, degreased in acetone, cleaned ultrasonically in distilled water and dried in air. After painting the solution with brush, the plates were treated at 670°C for 20 min in air, then the sample was extracted and left to cool. The operations were repeated until the required oxide

---

*Corresponding author.

E-mail address: pwang@icpm.syb.ac.cn (P. Wang).

0925-8388/00/$ – see front matter
PII: S0925-8388(00)00860-4

loading was attained. Finally, the electrodes were subjected to a final calcination of 5 h at the same temperature. The formation of the perovskite phase was checked by XRD.

The backside of the plate was contacted electrically with a nickel wire via silver paste and then painted with epoxy resin.

2.2. Surface characterization

The XPS analysis was performed using a LAS-3000 surface analysis instrument. For surface excitation, a Al anode X-ray source operating at 30 W was used. Spectrometer calibration was done with reference to C1s spectra. The base pressure inside the spectrometer during analysis was better than 2×10^{-7} Pa.

The electrochemical experiments were performed in a three-compartment glass cell at 25°C. A bright platinum foil was used as a counter electrode. The reference electrode was Hg/HgO/1 mol/1 KOH. Cyclic voltammetry study was carried out using E&G PARC MODEL 273A potentiostat controlled by a 386 computer.

3. Results and discussion

3.1. XPS surface analysis

Fig. 1 shows the survey spectra for $La_{1-x}Sr_xCoO_{3-\delta}$ series perovskites. The characteristic lines for La, Sr, Co and O are present.

The La $3d_{5/2}$ core level spectra of $La_{1-x}Sr_xCoO_{3-\delta}$ series perovskites with $x=0$ and 0.2 are shown in Fig. 2. The main peak of the La $3d_{5/2}$ spectra show two peaks situated at binding energy of 834.3 eV and 837.5 eV respectively duo to the presence of inequivalent La atoms. A weak satellite band appeared on the high binding energy side of the spectra. It is clear that the effect of the substitution of La by Sr on the chemical state of La is small from the shape and binding energy of the La $3d_{5/2}$ bands. Fig. 3 shows the Sr $3d_{5/2}$ spectra for the $La_{1-x}Sr_xCoO_{3-\delta}$ perovskites. Substitution of Sr for La shifts the binding energy of Sr $3d_{5/2}$ to more positive side. From the binding energy of the Sr $3d_{5/2}$ peak, we can identify it as Sr^{2+}. For the Co $2P_{3/2}$ spectra given in Fig. 4, a main peak at ca. 780. 1 eV accompanied by a weak satellite shoulder at ca. 789. 6 eV is present. The weak shake-up peak indicates the presence of low spin Co^{III} on the oxide surface [11]. The low spin Co^{III} with a binding energy of ca. 780. 1 eV is attributed to octahedral Co^{3+} [12]. For the $SrCoO_{3-\delta}$ system, a small shoulder presenting on the high binding energy side of the Co $2P_{3/2}$ spectra at ca. 786 eV can be identified as Co^{4+}. Considering the intensity of peaks, Co presented mainly as Co^{3+} and others Co^{4+} after substituting of Sr for La. O1s spectra given in Fig. 5. The analysis of the O1s core level spectra shows

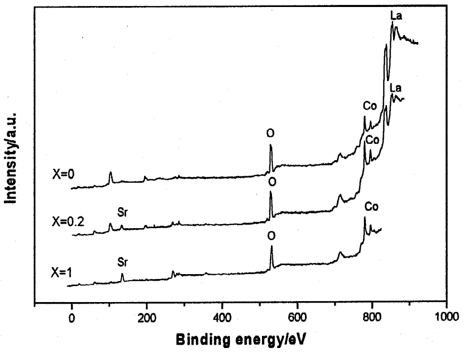

Fig. 1. Survey XPS spectra of the $La_{1-x}Sr_xCoO_{3-\delta}$ series perovskite oxides.

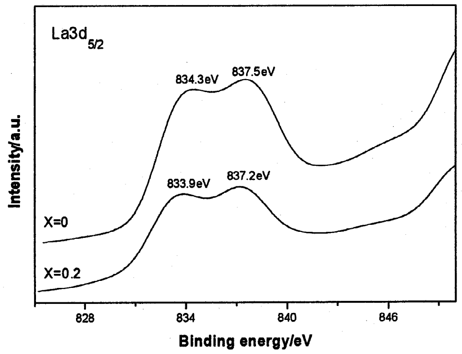

Fig. 2. La $3d_{5/2}$ spectra for $La_{1-x}Sr_xCoO_{3-\delta}$ with $x=0$ and 0.2.

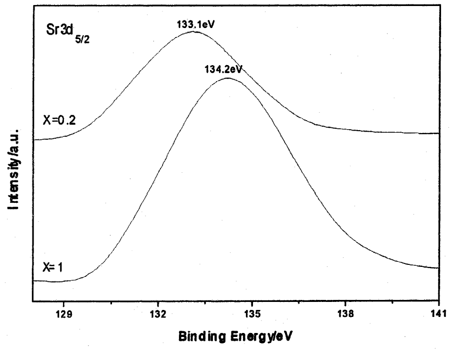

Fig. 3. Sr $3d_{5/2}$ spectra for $La_{1-x}Sr_xCoO_{3-\delta}$ with $x=0.2$ and 1.

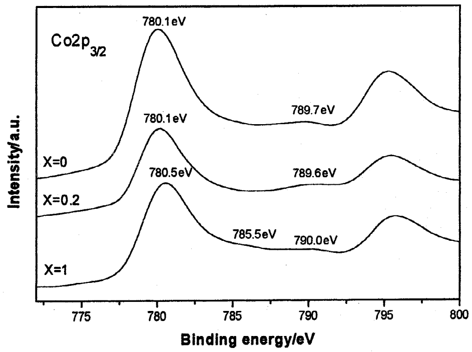

Fig. 4. Co $2P_{3/2}$ spectra for $La_{1-x}Sr_xCoO_{3-\delta}$ with $x=0$, 0.2 and 1.

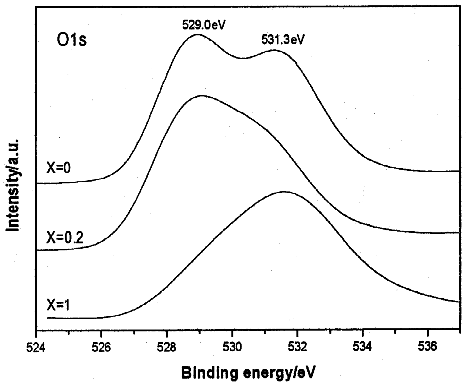

Fig. 5. O1s spectra for $La_{1-x}Sr_xCoO_{3-\delta}$ with $x=0$, 0.2 and 1.

that it is composed of two peaks, indicating two types of oxygen present on the electrode surface. The line at ca. 528. 6 eV is assigned to the oxygen in the lattice and the one at ca. 531.3 eV, to adsorbed oxygen-containing species [13,14]. Concerning the O1s spectra with different Sr content, it is clear that the lattice oxygen decrease with the Sr content indicating the increase of oxygen vacancies. The results of XPS show that some of Co^{3+} change to Co^{4+} and oxygen vacancies are formed as a result of the substitution of Sr for La.

3.2. Cyclic voltammetry

Fig. 6 shows the cyclic voltammograms for the $La_{1-x}Sr_xCoO_{3-\delta}$ electrodes in 1 mol/1 KOH. It is clear that the peak current increases, the anodic peak potential shifts to more positive potential and the cathodic peak potential shifts to more negative potential with the increase of Sr content. A couple of redox peaks appear at ca. 500 mV in the case of electrodes with high Sr content. It is reported that no electrochemical reaction occur on the $La_{1-x}Sr_xCoO_{3-\delta}$ electrodes in the anodic potential region, except for the anodic evolution of oxygen [15]. So the redox peaks at ca. 320 mV and ca. 450 mV for the oxide film on Ni can be ascribed to the presence of nickel ions in the catalytic film. The latter metal ions were dispersed in the film as a result of diffusion during the annealing process [16]. The couple of the redox peaks which appeared at ca. 320 mV and ca. 450 mV can be assigned to the redox reaction of Ni^{4+}/Ni^{3+} [17]. For the reaction:

$$CO_2 + H_2 + e^- \rightarrow CoOOH + OH^- \tag{1}$$

its E^0 is 0. 41 V (SCE) in alkaline solution [18]. So the redox peaks at ca. 500 mV are assigned to Co^{4+}/Co^{3+} surface redox reaction [19], which indicates that some of Co^{3+} change to Co^{4+} with the increase of Sr in $La_{1-x}Sr_xCoO_{3-\delta}$. The plateau oxidation current observed prior to the anodic peak is assigned to the following oxidation reaction of the electrode [20].

$$La_{1-x}Sr_xCoO_{3-\delta} + 2\delta\, OH^- \rightarrow La_{1-x}Sr_xCoO_3 + \delta\, H_2O + 2\,\delta\, e^- \tag{2}$$

which indicates that the oxygen ion vacancies formed on the oxide surface region are filled with oxygen ion in the OH^- by the above electrochemical reaction. From the trend of the plateau oxidation current with different Sr content, it is observed that the plateau oxidation current increases with x in $La_{1-x}Sr_xCoO_{3-\delta}$ which means that the density of oxygen vacancies increases with x. This is in line with the results obtained by XPS.

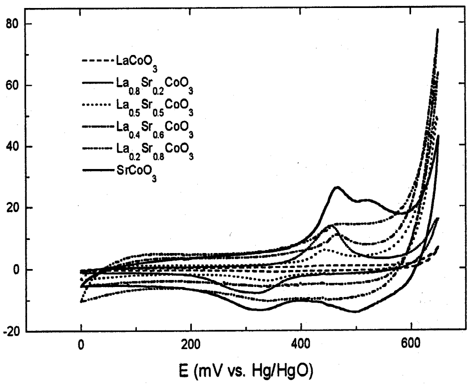

Fig. 6. Cyclic voltammograms for $La_{1-x}Sr_xCoO_{3-\delta}$ on Ni at scan rate of 20 mV/s in 1 mol/1 KOH (25°C).

4. Conclusions

The study has shown that the $La_{1-x}Sr_xCoO_{3-\delta}$ perovskite oxides are defect compounds and the substitution of Sr for La can modify their electronic structure. The results indicate that some of cobalt in the oxides change from low valence state Co^{3+} to high valence state Co^{4+} and high density of oxygen vacancies are formed as a result of the substitution of Sr for La.

References

[1] J. Mizusaki, J. Tabuchi, T. Matsuura et al., J. Electrochem. Soc. 136 (1989) 2082.
[2] J.G. McCarty, H. Wise, Catalysis Today 8 (1990) 231.
[3] N.Q. Minh, J. Am. Ceram. Soc. 76 (1993) 563.
[4] H.J.M. Bouwmeester, H. Kruidhof, A.J. Burggraaf, Solid State Ionics 72 (1994) 185.
[5] T. Arakawa, H. Kurachi, J. Shiokawa, J. Mater. Sci. 4 (1985) 1207.
[6] E.L. Brosha, B.W. Chung, F.H. Garzon et al., J. Electrochem. Soc. 142 (1995) 1702.
[7] M.H.R. Lankhorst, H.J.M. Bouwmeester, J. Electrochem. Soc. 144 (1997) 1261.
[8] M.H.R. Lankhorst, H.J.M. Bouwneester, J. Electrochem. Soc. 144 (1997) 1268.
[9] M.H.R. Lankhorst, H.J.M. Bouwmeester, H. Verweij, J. Solid State Chem. 133 (1997) 555.
[10] J.B. Goodenough, in: Progress in Solid State Chemistry, Vol. 5, Pergamon Press Ltd, Oxford, 1971, p. 145.

[11] D.C. Frost, C.A. McDowell, I.S. Woosley, Chem. Phys. Lett. 17 (1972) 320.
[12] G. Li, L. Dai, D. Lu, S. Peng, J. Solid State Chem. 89 (1990) 167.
[13] A.C. Tavares, M.I. Silva Pereira, M.H. Mendonca et al., J. Electroanal. Chem. 449 (1998) 91.
[14] J. Haenen, W. Visscher, E. Barendrecht, J. Electroanal. Chem. 208 (1986) 297.
[15] Y. Matsumoto, H. Manabe, E. Sato, J. Electrochem. Soc. 127 (1980) 811.
[16] A.N. Jain, S.K. Tiwari, J. Chem. Soc. Faraday Trans. 91 (1995) 1871.
[17] Y. Matsumoto, H. Yoneyama, H. Tamura, J. Electroanal. Chem. 80 (1977) 115.
[18] M. Pourbaix, Atlas of Electrochemical Equilibria in Aqueous Solutions. 2nd Edition, National Association of Corrosion Engineers, Houston, TX, 1974.
[19] R. Boggio, A. Carugati, S. Trasatti, J. Appl. Electrochem. 17 (1987) 828.
[20] Y. Matsumoto, S. Yamada, T. Nishida, E. Sato, J. Electrochem. Soc. 127 (1980) 2360.